High-spin level structure of ^{115}Rh: Evolution of triaxiality in odd-even Rh isotopes

S. H. Liu, J. H. Hamilton, A. V. Ramayya, A. Gelberg, L. Gu, E. Y. Yeoh, S. J. Zhu, N. T. Brewer, J. K. Hwang, Y. X. Luo, J. O. Rasmussen, W. C. Ma, A. V. Daniel, Yu. Ts. Oganessian, and G. M. Ter-Akopian

Phys. Rev. C **84**, 014304 — Published 7 July 2011

DOI: 10.1103/PhysRevC.84.014304

High-spin level structure of ^{115}Rh: evolution of triaxiality in odd-even Rh isotopes

S. H. Liu,[1,2] J. H. Hamilton,[1] A. V. Ramayya,[1] A. Gelberg,[3] L. Gu,[4] E. Y. Yeoh,[4] S. J. Zhu,[4] N. T. Brewer,[1] J. K. Hwang,[1] Y. X. Luo,[1,5] J. O. Rasmussen,[5] W. C. Ma,[6] A. V. Daniel,[1,7] Yu. Ts. Oganessian,[7] and G. M. Ter-Akopian[7]

[1] *Department of Physics and Astronomy, Vanderbilt University, Nashville, Tennessee 37235, USA*

[2] *UNIRIB/Oak Ridge Associated Universities, Oak Ridge, Tennessee 37831, USA*

[3] *Institut für Kernphysik, Universität zu Köln, 50937 Cologne, Germany*

[4] *Department of Physics, Tsinghua University, Beijing 100084, People's Republic of China*

[5] *Lawrence Berkeley National Laboratory, Berkeley, California 94720, USA*

[6] *Department of Physics and Astronomy, Mississippi State University, Mississippi State, Mississippi 39762, USA*

[7] *Joint Institute for Nuclear Research, RU-141980 Dubna, Russian Federation*

(Dated: May 20, 2011)

High-spin excited states in the neutron-rich nucleus ^{115}Rh have been identified for the first time by studying prompt γ rays from the spontaneous fission of ^{252}Cf with the Gammasphere detector array. A new yrast band and a side-band are built in ^{115}Rh. This level scheme is proposed to be built on the $7/2^+$ ground state. The existence of a large signature splitting and an yrare band in ^{115}Rh shows typical features of a triaxially deformed nucleus. The Rigid Triaxial Rotor plus Particle model is used to interpret the level structure of ^{115}Rh. The level energies, gamma branching ratios, the large signature splitting in the yrast band, and the inverted signature splitting in the yrare band in ^{115}Rh are reproduced very well. Strong K-mixing occurs in ^{115}Rh at high spin.

PACS numbers: 27.60.+j, 23.20.Lv, 21.60.Ev, 25.85.Ca

I. INTRODUCTION

The $Z = 45$ neutron-rich Rh isotopes are located in a region where nuclei are characterized by shape coexistence and shape transitions, including triaxial shapes [1]. In this region, the proton orbitals originating from the $\pi g_{9/2}$ sub-shell are influenced by the triaxial deformation. The appearance of triaxial deformations and soft shape transitions has been found in nuclei of $Z \geq 42$ [2, 3]. Our previous systematic studies of neutron-rich, odd-even Y, Nb, Tc, and Rh ($Z = 39, 41, 43, 45$) isotopes indicated a shape transition from axial symmetry with large quadrupole deformations in ^{99,101}Y to a deformed shape with large triaxiality in ^{107,109,111}Tc and ^{111,113}Rh [4–7].

In a ground state with $Z = 45$, the valence protons occupy hole-like states in the $Z = 50$ closed shell, with a main configuration $\pi 1g^5_{9/2}$. The valence neutrons occupy mainly particle-like states in the $50-82$ shells. Due to the proton-neutron interaction, the nucleus is deformed, with a tendency to triaxiality. Rotational bands built on $\pi g_{9/2}$, $\pi p_{1/2}$ and $\pi(g_{7/2}/d_{5/2})$ sub-shells have been observed in odd-even $^{107-113}$Rh [7–9]. The existence of an yrare band built on an $11/2^+$ excited state and a large signature splitting in the yrast band in ^{107,109,111,113}Rh provides evidence for triaxiality, which has been confirmed by theory. Theoretical calculations based on the rigid-triaxial-rotor-plus-particle (RTRP) model provided a reasonable fit to excitation energies and branching ratios of the yrast bands and the collective yrare bands as well as to the signature splittings in the yrast bands of ^{111,113}Rh at near-maximum triaxiality with $\gamma = 28°$ [7], larger than $\gamma = 23°$ for ^{107}Rh [8]. Thus, it is of interest to study the structure evolution of odd-even Rh to the more neutron-rich region. Low-lying excited states in ^{115}Rh were reported in Ref. [10] through β-decay studies of ^{115}Ru and $7/2^+$ was assigned to the ground state of ^{115}Rh [11]. Here, we report the first high-spin level scheme of the very neutron-rich nucleus ^{115}Rh ($N = 70$).

II. EXPERIMENTS AND RESULTS

This work was done by examining the prompt γ-rays emitted from the spontaneous fission of ^{252}Cf. Data were obtained with the Gammasphere array at Lawrence Berkeley National Laboratory. A ^{252}Cf spontaneous fission source of 62 μCi was sandwiched between two iron foils of 10 mg/cm^2, which were used to stop the fission fragments and eliminate the need for a Doppler correction. A plastic ball of 7.62 cm in diameter, surrounding the source, was used to absorb β rays and conversion electrons, as well as to partially moderate and absorb fission neutrons. A total of 5.7×10^{11} triple- and higher-fold γ-ray coincidence events were recorded. Data were analyzed with the RadWare software package [12].

The level scheme of ^{115}Rh established in the present work is shown in Fig. 1. One clearly sees that the energy of the strongest transition in ^{115}Rh is very close to the strongest 211.7-keV transition in ^{111}Rh and ^{113}Rh [7] with much larger fission yields than ^{115}Rh and the 211.2-keV transition in ^{114}Rh [13]. So one highlight of the present work is the separation of the four peaks, the 211.7 keV in ^{111,113}Rh, the 211.2 keV in ^{114}Rh, and the 213.3 keV in ^{115}Rh, in the spectra with gates set on transitions in their iodine partners.

The identifications of the transitions in ^{115}Rh were based on extensive cross-checking of the coincidence relationships and relative intensities among transitions in its complementary fission fragments $^{133-135}$I [14–16]

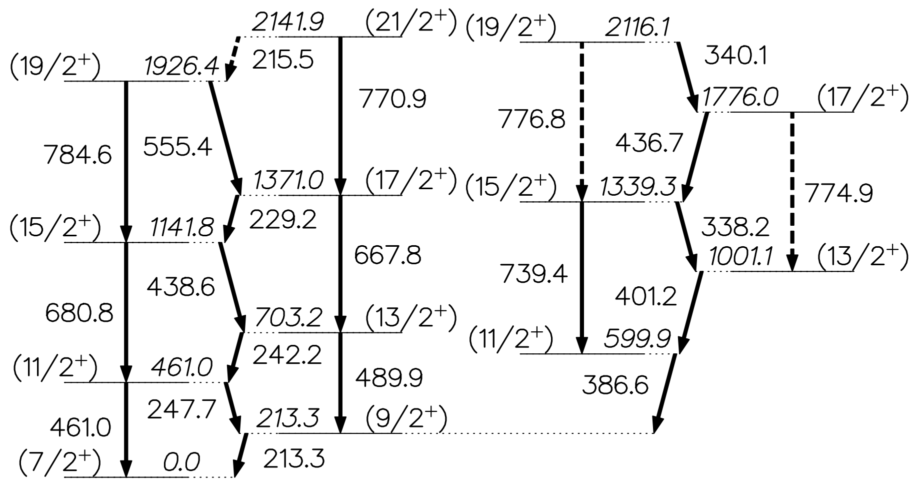

FIG. 1. A high-spin level scheme of ^{115}Rh built in the present work. All transitions are newly observed. Uncertainties of transition energies are about 0.3 keV.

and itself. Careful background subtractions were always performed to eliminate possible accidental coincidences. Several coincidence spectra were created by double-gating on strong transitions in $^{133-135}$I and new ones assigned to ^{115}Rh to show evidence for the identifications of new transitions in ^{115}Rh.

Two spectra were obtained by double-gating on two transitions in ^{134}I and ^{135}I where a new transition of energy 247.7 keV is seen in both spectra, along with those previously known strong transitions in $^{111-114}$Rh [7, 9, 13]. Three spectra were obtained by double-gating on the new 247.7-keV transition and a strong transition in each of ^{133,134,135}I, respectively, as shown in Fig. 2. Two new transitions of energies 213.3 and 242.2 keV are seen in these spectra in Fig. 2. The 211.7-keV transition in ^{113}Rh and the new 213.3-keV transition form a doublet peak in Fig. 2 (c) because of the large fission yield of ^{113}Rh, 4-n fission partner of ^{135}I. The spectra gated on the new 213.3-keV transition and on the 912.7- (^{133}I), 952.4- (^{134}I), and 1133.8-keV (^{135}I) transitions, respectively, clearly demonstrate the coincidence relationships among the new 213.3-, 242.2-, and 247.7-keV transitions as well as those in the I isotopes, as presented in Fig. 3. One new transition of energy 489.9 keV, equal to the sum of 242.2 and 247.7 keV, is coincident with the 213.3-keV transition. A new transition of energy 386.6 keV is observed in Fig. 3, but not coincident with the new 247.7-keV transition. So the new 386.6-keV transition, in coincidence with the new 213.3-keV transition and the transitions in the I isotopes, should be in another band in this Rh nucleus, which is supported by observing the 213.3.-keV transition and two new transitions of energies 338.2 and 401.2 keV in the spectra double-gated on the new 386.6-keV transition and on the 912.7- (^{133}I), 952.4- (^{134}I), and 1133.8-keV (^{135}I) transitions. Three spectra gated on the new 213.3- and 247.7-keV transitions, the new 242.2- and 247.7-keV transitions, and the new 386.6- and 338.2-keV transitions, respectively, as shown in Fig. 4, indicate the coincidence relationships among the newly observed transitions and known ones in $^{133-135}$I. These coincidence data enable us to establish a new level and assign it to a single Rh isotope, as shown in Fig. 1.

As seen in the above spectra, the transitions in the level scheme shown in Fig. 1 are in coincidence with transitions in I isotopes. Therefore, we propose the level scheme in Fig. 1 belongs to ^{115}Rh since the level schemes of $^{111-114}$Rh have been known. The most crucial support comes from the following measurements to determine the mass number of these transitions. In the 60.6/183.0- (^{112}Rh), 232.2/240.6- (^{113}Rh), 195.9/264.1- (^{114}Rh), and 213.3/247.7-keV double-gates, the fission yield ratios of the 1133.8-keV transition in ^{135}I to the 952.4-keV transition in ^{134}I were measured as 13.9(19), 5.63(79), 3.80(53), and 1.92(27), respectively. The variation of these ratios is very similar to those of ^{142}Cs to ^{141}Cs in the $^{105-108}$Tc gates, as presented in Fig. 5. Therefore, we conclude that the 247.7 $\rightarrow$ 213.3-keV cascade is in ^{115}Rh after considering the fact that the fission yield of ^{115}Rh is much greater than those of other heavier Rh isotopes in the ^{252}Cf fission. The same ratio in the 213.3/386.6-keV gate was also measured to be 1.97(28), which is consistent with the value in the 213.3/247.7-keV gate. So the 401.2 $\rightarrow$ 386.6-keV cascade forms a side-band in ^{115}Rh, as shown in Fig. 1.

Because of the severe overlap of the 211.7-keV tran-

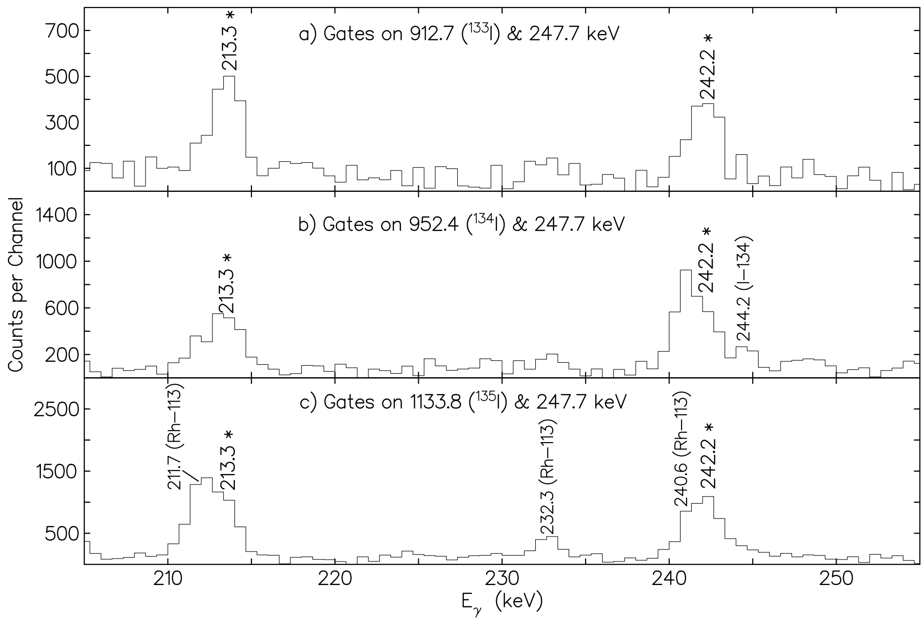

FIG. 2. Coincidence spectra double-gated on the newly observed 247.7-keV transition and the 912.7- (^{133}I), 952.4- (^{134}I), and 1133.8-keV (^{135}I) transitions. Two new transitions of energies 213.3 and 242.2 keV are seen and marked with an asterisk. Contaminations from ^{113}Rh [7] in (c) are caused by the 247.7-keV transition which is close to the 244.5-keV transition in ^{113}Rh.

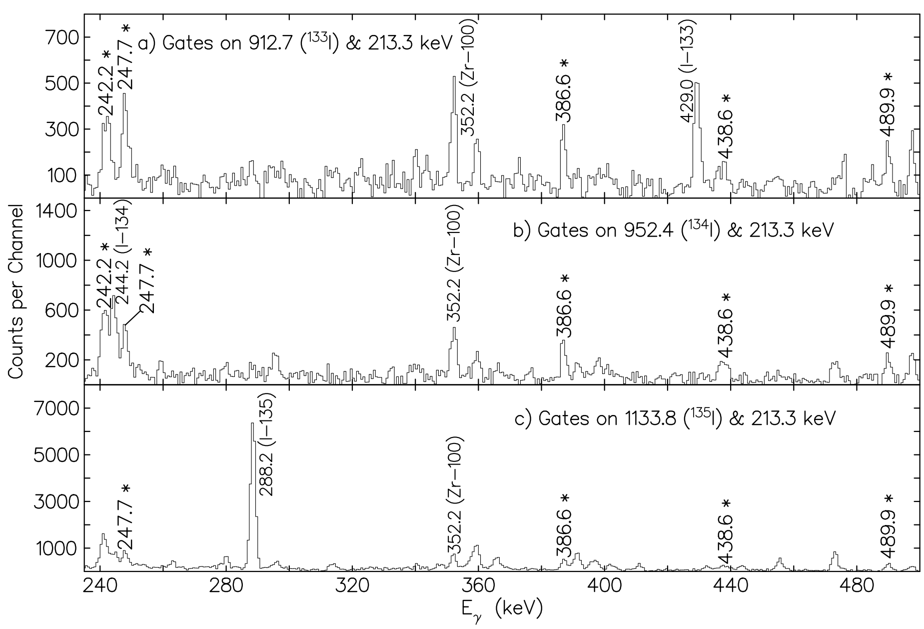

FIG. 3. Coincidence spectra double-gated on the new 213.3-keV transition and the 912.7- (^{133}I), 952.4- (^{134}I), and 1133.8-keV (^{135}I) transitions. The new 489.9-, 386.6-, and 438.6-keV transitions are marked with an asterisk. The strongest 212.6-keV transition in ^{100}Zr [17], close to 213.3 keV, leads to the contamination of the 352.2-keV peak in ^{100}Zr [17] in these spectra.

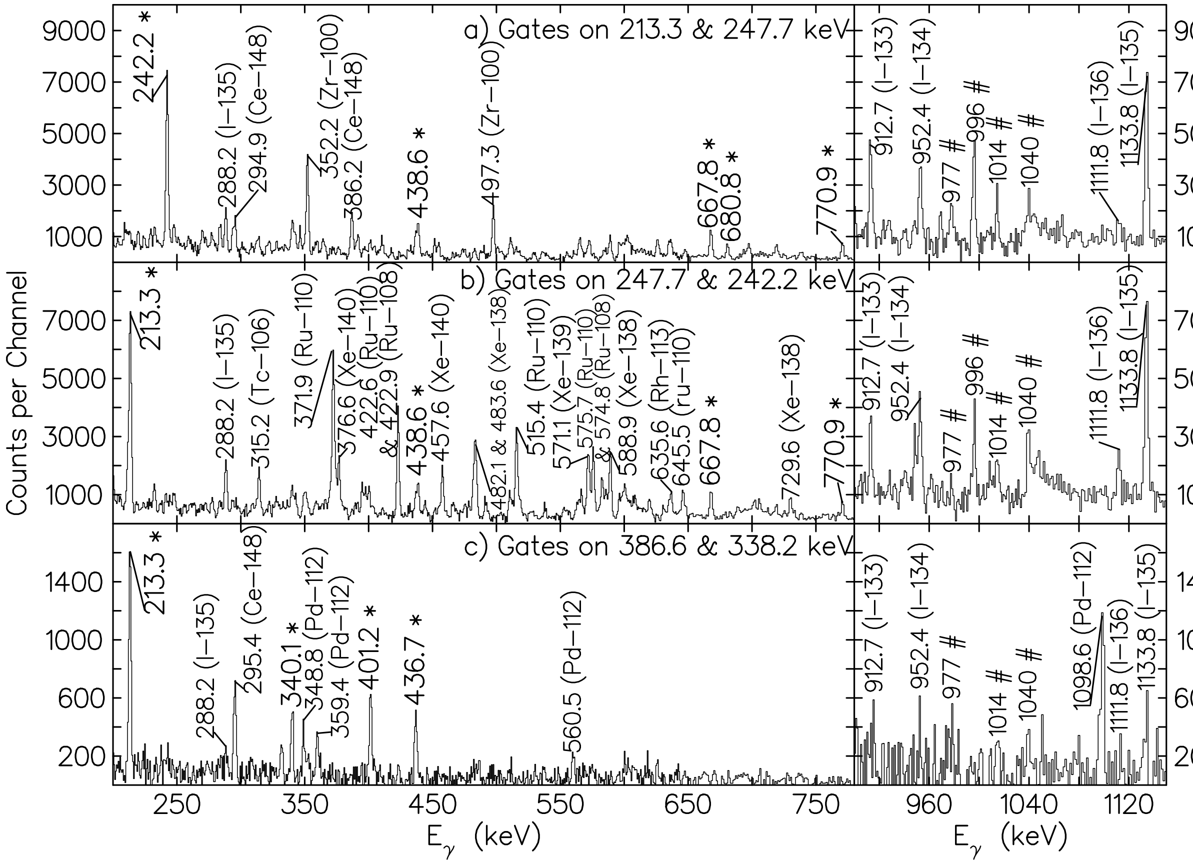

FIG. 4. Coincidence spectra double-gated on the new 213.3- and 247.7-keV transitions, the new 247.7- and 242.2-keV transitions, and the new 386.6- and 338.2-keV transitions. All coincidence transitions marked with an asterisk are newly observed. The strongest 212.6-keV transition in ^{100}Zr [17], close to 213.3 keV, leads to the contamination of the 352.2- and 497.3-keV peaks in ^{100}Zr [17] and the 294.9- and 386.2-keV peaks in ^{148}Ce [18] in (a); In (b), contaminations from ^{108,110}Ru [19] and ^{138,139,140}Xe [20] caused by the strongest 242.3-keV transition in ^{108}Ru and the strongest 240.8-keV transition in ^{110}Ru are labeled along with the 315.2-keV peak in ^{106}Tc [21] and the 635.6-keV peak in ^{113}Rh [7] which are caused by the strong 241.9-keV transition in ^{106}Tc and the strong 240.6-keV transition in ^{113}Rh, respectively; In (c), contaminations from ^{148}Ce [18] and ^{112}Pd [22] are indicated which are caused by the 386.2-keV transition in ^{148}Ce and the strong 388.0-keV transition in ^{112}Pd, respectively. In the high-energy region, background peaks are labeled with a pound sign.

sition in ^{113}Rh and the 211.2-keV transition in ^{114}Rh and weak population of ^{115}Rh in the ^{252}Cf fission, only γ branching ratios for some levels were measured for further discussion in Section IV, instead of the relative transition intensities.

III. DISCUSSION

The high-spin level scheme of ^{115}Rh provides very useful information for exploring the structure evolution of the odd-even Rh isotopic chain to the more neutron-rich region. Though the level scheme of ^{115}Rh was not observed up to high spins as in the lighter odd-even Rh isotopes, due to its low fission yield, we still can obtain sufficient data to make valuable conclusions, which will be discussed in this section.

A. Excitation Energies

The level structure of ^{115}Rh, as presented in Fig. 1, bears significant resemblance to bands 1 and 6 of ^{107,109}Rh [8, 9] and ^{111,113}Rh [7, 9] that are built on the $\pi g_{9/2}$ sub-shell. The identified levels in ^{115}Rh do not reach such high spins as those in ^{111}Rh and ^{113}Rh; only two bands were observed in ^{115}Rh, fewer than in ^{107,109,111,113}Rh. We proposed that the present level

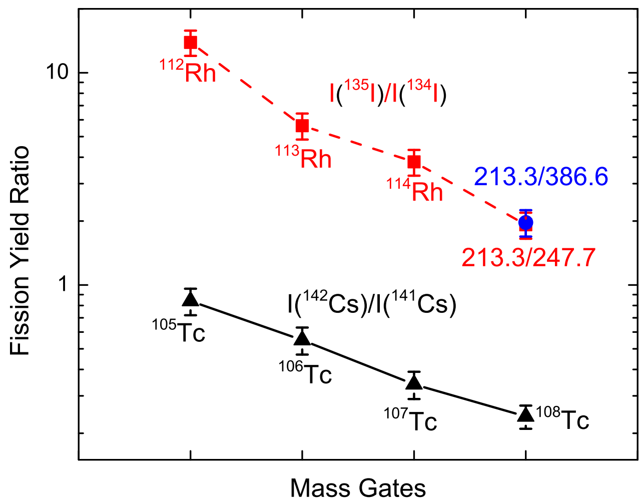

FIG. 5. (Color online) Fission yield ratios of ^{135}I to ^{134}I in Rh gates and those of ^{142}Cs to ^{141}Cs in Tc gates. Data are taken from Refs. [5, 7, 15, 16, 21, 23–25] and the present work. A logarithmic scale is used for the y-axis.

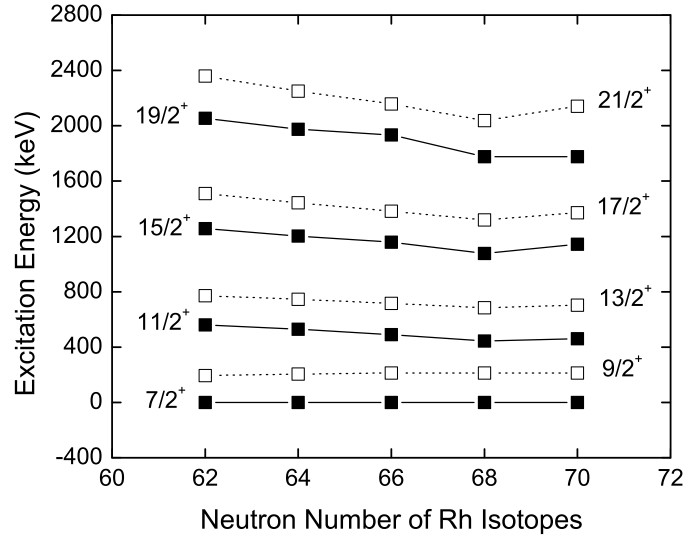

FIG. 6. Systematics of level energies in the yrast bands of odd-even $^{107-115}$Rh. Excitation energies decrease towards $N = 68$ and after that increase. Data are taken from Refs. [7–9] and the present work.

scheme of ^{115}Rh is built on the $7/2^+$ ground state and we assigned spin-parities to other higher levels based on systematics and their yrast and high-spin features. A side-band strongly populating the yrast $9/2^+$ excited level has been observed in ^{115}Rh, as in ^{107,109,111,113}Rh, whose features indicate a deviation from axial symmetry. $11/2^+$ was assigned to its band-head and $13/2^+$, $15/2^+$, $17/2^+$, and $19/2^+$ to other higher states. In Ref. [26], the study on ^{125}Xe shows that the signature pattern of the yrast band could appear in two triaxial shapes, either on the prolate side or the oblate side. The side-band, the so-called yrare band, can be used to determine on which side the triaxial shape is on. The side-band in the Xe isotope is analogous to the side-band here in ^{115}Rh, as confirmed in ^{111,113}Rh in Ref. [7]. In the following model calculations, level energies in ^{115}Rh are well reproduced as natural consequences of the triaxial deformation (See Section IV).

Figure 6 shows the systematics of the long odd-even Rh isotopic chain from ^{107}Rh to ^{115}Rh. Level energies of the yrast bands of these Rh nuclei are compared and a trend that excitation energies decrease with increasing neutron numbers is observed before the neutron number reaches 68. The same $N = 68$ effect is seen in neighboring Ru and Pd isotopes as well, when we look at excitation energies of the yrast bands of even-even $^{102-114}$Ru and $^{106-120}$Pd. It is worth pointing out that finding a similar effect in the Rh isotopes as assigned additionally supports our mass number and spin-parity assignments. It is also interesting to investigate the systematics of excitation energies of the yrare bands in these Rh isotopes. In Fig. 7, the level energies up to the $15/2^+$ state in the yrare bands relative to the $7/2^+$ ground state in odd-even $^{107-115}$Rh are plotted. The above mentioned $N = 68$ effect is seen again in the yrare bands in the Rh isotopes.

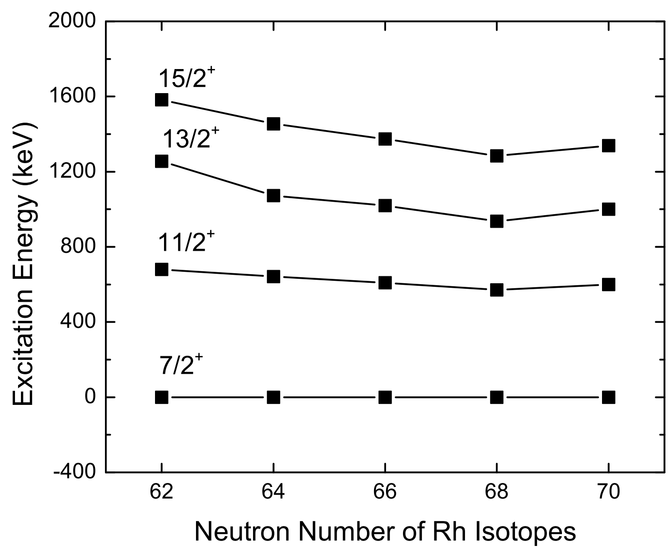

FIG. 7. Systematics of level energies in the yrare bands of odd-even $^{107-115}$Rh. Excitation energies decrease towards $N = 68$ and after that increase in Rh isotopes. Data are taken from Refs. [7–9] and the present work.

B. Backbending

In Ref. [7], Luo *et al.* reported the observation of back-bending in the yrast bands of ^{111,113}Rh that sets in above the $21/2^+$ level in ^{111}Rh and the $19/2^+$ level in ^{113}Rh. Therefore, it is of interest to find if the back-bending occurs in ^{115}Rh. Figure 8 is a back-bending plot (kinetic moment of inertia vs rotational frequency) for the yrast bands of $^{108-115}$Rh. A back-bending is clearly seen in ^{109}Rh, ^{111}Rh, and ^{113}Rh and the back-bending frequency moves monotonically higher with decreasing neutron numbers. For ^{115}Rh, its kinetic moment of inertia at low rotational frequency is comparable to those for ^{109}Rh, ^{111}Rh, and ^{113}Rh. One cannot determine where a back-bending occurs in ^{115}Rh because levels in ^{115}Rh identified here are not as high as in ^{109,111,113}Rh. However, one may predict that the back-bending frequency in ^{115}Rh, which is obviously higher than that in ^{113}Rh, is either comparable to or higher than that in ^{111}Rh or higher than even that in ^{109}Rh, by following the data shown in Fig. 8. It is very interesting to see that the back-bending in ^{115}Rh does not conform to the above systematics in ^{109}Rh, ^{111}Rh, and ^{113}Rh, where the back-bending frequency systematically decreases ingoing from ^{109}Rh to ^{113}Rh. More experimental work is needed to find the accurate back-bending frequency and further theoretical work is required to interpret the above observation if it is correct. Data for the odd-odd $^{108-114}$Rh are also included in Fig. 8, where no back-bending is found. The lack of back-bending in ^{108,110,112,114}Rh could be blocked by the odd neutron. So, the back-bending in ^{109}Rh, ^{111}Rh, and ^{113}Rh means a neutron pair breaking in these odd-even Rh isotopes. As mentioned in Ref. [7], the breaking pair is in the $h_{11/2}$ neutron orbital.

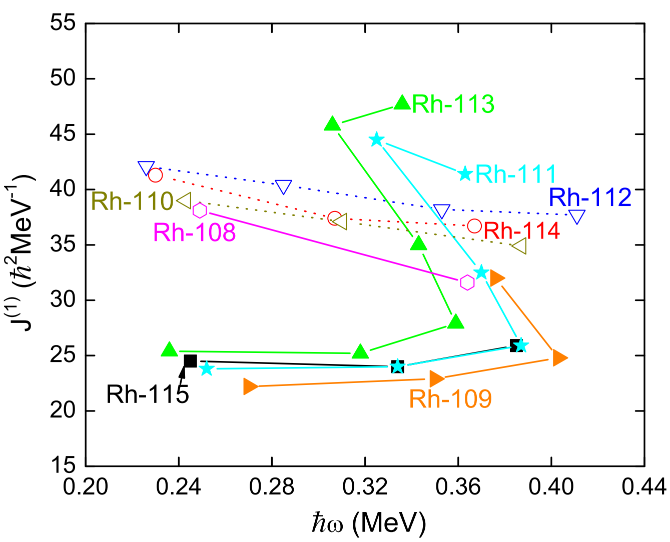

FIG. 8. (Color online) Kinetic moment of inertia vs frequency for the $\alpha = +1/2$ signature partners of the yrast bands of odd-even $^{108-115}$Rh and the even-integer signature partners of the yrast bands of odd-odd $^{108-115}$Rh. Back-bending is observed in ^{109,111,113}Rh. Data are taken from Refs. [7, 13, 27] and the present work.

C. Signature Splitting

The signature splitting is familiar from cranking calculations. It manifests itself through deviations of excitation energies in a band, from the simple strong coupling $I(I+1)$ rule. It can be used as an indicator of the shape of the nucleus. A few features of the signature splitting will be discussed in Section IV A. The triaxial deformation can contribute to a large signature splitting, because K is not a good quantum number any longer. Here, the plots for the signature splittings in the yrast bands of odd-even $^{107-115}$Rh are presented in Fig. 9, where the signature splitting function $S(I)$, which is extremely sensitive to the triaxial deformation parameter γ, is defined as [28, 29]

$$S(I) = \frac{E(I) - E(I-1)}{E(I) - E(I-2)} \frac{I(I+1) - (I-2)(I-1)}{I(I+1) - (I-1)I} - 1. \tag{1}$$

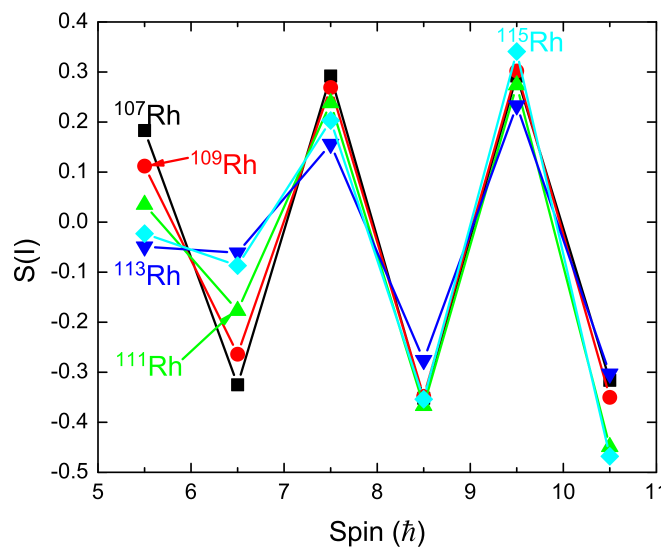

FIG. 9. (Color online) Signature splitting function $S(I)$ for the yrast bands of odd-even $^{107-115}$Rh. Data are taken from Refs. [7–9] and the present work.

One sees that the signature splitting of ^{115}Rh is basically comparable to those of ^{107,109,111,113}Rh. This feature provides additional support for our mass number and spin-parity assignments. As shown in Fig. 9, a very large signature splitting in the yrast band is observed in ^{115}Rh. The splitting pattern in ^{115}Rh is similar to those in ^{107,109,111,113}Rh and all of these five Rh isotopes have a likeness in the splitting strength at high spin. Such large signature splittings observed in ^{107,111,113}Rh have been interpreted in Refs. [7, 8] in terms of triaxiality playing a major role. One also finds a large signature splitting in the neighboring Ag isotopes, ^{115}Ag and ^{117}Ag, as plotted in Fig. 10. The signature splitting in the Ag isotopes is even greater than that in their corresponding Rh isotones, which may indicate that the K-mixing caused by triaxiality in these Ag isotopes is larger than that in the corresponding Rh isotones. Gamma-softness in ^{115,117}Ag was proposed in Ref. [30].

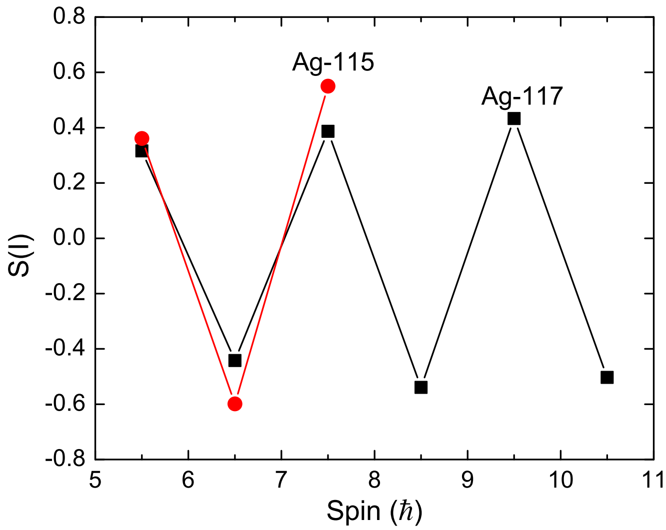

FIG. 10. (Color online) Signature splitting function $S(I)$ for the yrast bands of odd-even ^{115,117}Ag. Data are taken from Ref. [30].

It is interesting to find that the γ values are 19°, 15°, and 13° in ^{101,103,105}Nb [4], respectively, decreasing with increasing neutron numbers, following the variation of their signature splittings. However, in ^{107,109,111}Tc, their signature splittings increase slowly with increasing neutron numbers with $\gamma = 22.5°$, 25°, and 26°, giving the best fit of their data, respectively [5, 6]. Again, in Rh isotopes with triaxiality, one sees increasing γ values with increasing neutron numbers from 23° for ^{107}Rh [8] to 28° for ^{111}Rh [7] with nearly maximum triaxiality. The γ values remain the same, namely 28°, from ^{111}Rh [7] to ^{113}Rh [7]. However, the difference between the signature splitting of ^{107}Rh and those of the heavier Rh isotopes like ^{111}Rh seems not be as distinct as that in ^{107,109,111}Tc shown in Fig. 11 in Ref. [6], especially at high spin. Furthermore, the signature splitting in ^{113}Rh is seen as the smallest one among ^{107,109,111,113,115}Rh, while the γ value for ^{113}Rh is almost identical to the values for ^{111,115}Rh (For ^{115}Rh, see Section IV). We also noticed that calculations based on the RTRP model in Ref. [7] did produce a larger splitting than experiment with $\gamma = 28°$. Thus, an interesting open question emerges concerning the trends of the γ values with the signature splitting and increasing neutron numbers. More experimental and theoretical efforts might be needed to answer it. It is worth pointing out that the quadrupole deformation in Tc remains exactly the same, while that in Nb and Rh varies slightly.

One also sees a decrease in the signature splitting from ^{107}Rh to ^{113}Rh somewhat at $I = 11/2$. The signature splitting at $I = 11/2$ then increases in ^{115}Rh. This phenomenon may be related to the $N = 68$ effect as discussed above. The signature splittings in ^{113,115}Rh are very small at low spin.

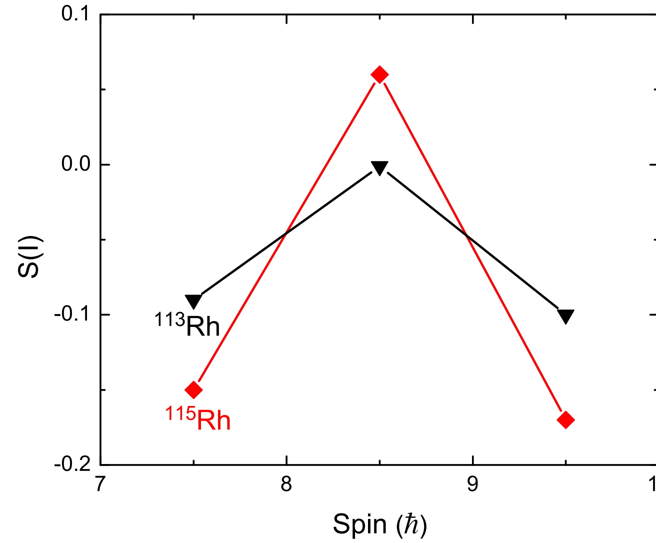

FIG. 11. (Color online) Anomalous signature splittings in the yrare bands of ^{113,115}Rh.

Let us then have a look at the signature splitting in the yrare band of ^{115}Rh, as shown in Fig. 11 where $S(I)$ vs spin in the yrare band of ^{113}Rh is included. For the $\pi g_{9/2}$ sub-shell, the signature formula $\alpha_\mathrm{f} = \frac{1}{2}(-1)^{j-1/2}$ gives $\alpha_\mathrm{f} = +\frac{1}{2}$. So the states with $I = 9/2$, $13/2$, $17/2$, $\cdots$ are favored, while those with $I = 7/2$, $11/2$, $15/2$, $\cdots$ are unfavored. Obviously, the 17/2 yrare favored state observed here in ^{115}Rh has a $S(I)$ larger (positive) value than the negative values of the unfavored states at 15/2 and 19/2 as seen in Fig. 11, which is opposite to what should occur in the strongly coupled case (also compare with Fig. 9). So these small signature splittings are inverted and anomalous with respect to what a cranking calculation predicted in the yrare bands of odd-even ^{113,115}Rh. It is interesting to see a connection between triaxiality and the signature inversion which has been discussed in Refs. [13, 31].

IV. ROTOR-PLUS-PARTICLE-MODEL CALCULATIONS

A. The Model

As shown in Section III, the strong signature splitting observed in ^{115}Rh, as well as in the ^{111,113}Rh isotopes, points to the presence of triaxial deformations. Moreover, the global calculations of nuclear ground states by Möller et al. [34] predict deviations from axial symmetry in a region around Ru. According to Ref. [35], ^{114}Ru shows properties characteristic for a rigid, triaxially deformed nucleus [36]. The triaxial rotor model [36] has been extended to odd-A nuclei ; it is known as the Rigid Triaxial Rotor plus Particle (RTRP) model. This model has been quite successful. In particular, it has been applied to ^{107}Rh [8] and ^{111,113}Rh [7].

The Hamiltonian contains a deformed single particle mean field, pairing, and a rotational term. The mean field is charcterized by the deformation parameters ϵ and γ. ϵ is the quadrupole deformation parameter, and γ is the triaxiality parameter. The details of the used model can be found in Refs. [37, 38]. The hydrodynamical moments of inertia are those given in Ref. [39]. A short description of the model is given in Ref. [7].

The main feature of the model is the strong K-mixing; K is the projection of the total angular momentum on the quantization axis. It is given by

$$K = \Omega + R_3 \quad (2)$$

where Ω and R_3 are the projections of the particle and rotation angular momenta, respectively. Contrary to the axially symmetric case, the rotation angular momentum can have a non-vanishing projection on the quantization axis. In the case that this happens, $K \neq \Omega$.

A triaxially deformed nucleus has an important discrete symmetry. The Hamiltonian commutes with the $R_x(\pi)$ operator of a 180° rotation around the intrinsic x-axis [39]. This allows the introduction of the sigantures quantum number. In the strong coupling approximation, the excitation energies of a band strictly obey the $I(I+1)$ rule, regardless of signature. The only exception is the $K = \frac{1}{2}$ band, in which the signature splitting clearly appears, as a result of the Coriolis force [39]. Signature splitting has been observed also in axially symmetric nuclei, in bands with $K > 1/2$. This is due to the $K(\Omega)$-mixing induced by the Coriolis interaction [39]. This signature splitting is rather small, especially in well deformed nuclei. If the nucleus is triaxially deformed, i.e. gamma does not vanish, the K-mixing increases, and the signature splitting is enhanced. Test calculations done at different values of gamma show that the signature splitting indeed increases with increasing gamma.

The signature splitting can be plotted through the $S(I)$ function [28, 29] (see Eq.(1)), which vanishes in the case of strong coupling. The Hamiltonian has been diagonalized by using the GAMPN, ASYRMO and PROBAMO codes [41].

B. Results

The parameters were first fitted to the excitation energies, which are mainly sensitive to ϵ and $E(2^+)$. The latter is connected to the moment of inertia parameter. As in previous calculations, the Coriolis matrix elements were reduced by a factor $\xi = 0.8$. In the next step, γ was fitted to the signature splitting. The values of the fitted parameters are $\epsilon = 0.26, \gamma = 27.5°$, and $E(2^+) = 0.31$ MeV. The fitted γ should be considered as only an effective value [40]. One may ask whether the fit could be improved by choosing a value of gamma located in the oblate region ($gamma > 30$). We tested this hypothesis in the case of ^{111}Rh in Ref. [7], but it was not possible to find a satisfactory value of gamma. For instance, we were not able to fit at the same time the excitation energies and the signature splitting. For some values of gamma, we got a $9/2^+$ ground state, which is wrong. Since ^{111}Rh and ^{115}Rh are quite similar, we did not repeat this test for the latter nucleus.

The calculated energies are given in Table I, where the corresponding experimental level energies are included as well for comparison. We consider the excitation energy fit as satisfactory.

TABLE I. Comparison of experimental and theoretical energies of excited states in the yrast band and the yrare band of ^{115}Rh. Energies are in keV. Experimental level energies are rounded to the nearest integer.

	Yrast band		Yrare band	
State	$E^{\rm exp}$	$E^{\rm theory}$	$E^{\rm exp}$	$E^{\rm theory}$
$7/2^+$	0	0		
$9/2^+$	213	132		
$11/2^+$	461	480	600	594
$13/2^+$	703	634	1001	1017
$15/2^+$	1142	1100	1339	1585
$17/2^+$	1371	1338	1776	2171
$19/2^+$	1926	2004	2116	2666
$21/2^+$	2142	2234		

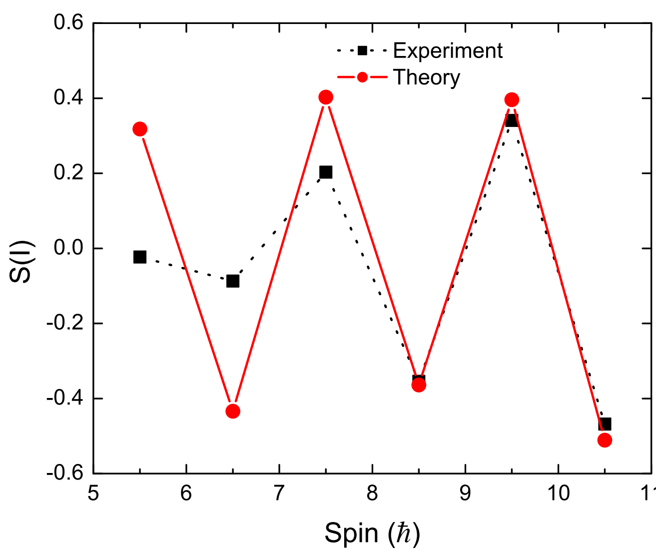

FIG. 12. (Color online) Comparison of experimental signature splitting in ^{115}Rh with theoretical results based on the RTRP model with $\gamma = 27.5°$.

The signature splitting of the yrast sequence can be seen in Fig. 12. An anomaly of the signature splitting at $I = 11/2$ and $13/2$ is seen. This feature is not reproduced by the calculation. The same anomaly is seen in the case of ^{113}Rh. One possible explanation would be a decrease of γ at low spin.

As mentioned in Section III B, the yrare signature splitting is inverted with respect to yrast in ^{115}Rh. The calculation gives $S(19/2_2) = -0.14$, compared with the experimental value $S(19/2_2) = -0.17$. Both experimental and calculated values of the yrast $S(19/2)$ are positive. It is difficult to discuss the yrare splitting, because it can be calculated only for $I = 15/2$, $17/2$, $19/2$ (The $S(I)$ formula contains 3 spins).

Three gamma branching ratios have been calculated and shown in Table II, together with the experimental values. The fit of the first two is satisfactory, while the third one shows a larger deviation. The transition $11/2_2 \rightarrow 7/2_1$ has not be observed in ^{115}Rh. The analogue transitions have been observed in ^{111,113}Rh, but they are quite weak. This has to do with the coupling of the particle, which is located on the $1g_{9/2}$ orbital, with the core. In both the $7/2_1$ ground state and the $11/2_2$ state, the particle is coupled mainly to the 2_1^+ excited state of the core. Since γ is very close to 30°, the diagonal quadrupole matrix element nearly vanishes. On the contrary, in the $9/2_1$ state, the particle is coupled to the 0_1^+ ground state of the core, and the $E2$ matrix elements to the $11/2_2$ and $7/2_1$ states are large. This feature indicates triaxial deformations.

TABLE II. Some γ branching ratios in the yrast band of ^{115}Rh.

Branch	Exp.	Calc.
$\frac{(11/2-9/2)}{(11/2-7/2)}$	1.69(20)	1.64
$\frac{(13/2-11/2)}{(13/2-9/2)}$	1.19(14)	0.87
$\frac{(15/2-13/2)}{(15/2-11/2)}$	1.72(20)	0.63

These are rather qualitative considerations. In reality, the particle is coupled to several core states, which have an amplitude distribution. The squared amplitudes (in %) can be seen in Table III for the states with spins $7/2_1$, $9/2_1$, $11/2_2$. One can notice that the $11/2_2$ state contains also a component with $R = 2_2$. The amplitudes have been calculated by using the code ASYRMOIR [42].

TABLE III. Core states probabilities in %. R is the core angular momentum.

R	0_1	2_1	2_2	3_1	4_1	4_2
$7/2_1$	0.4	64.0	8.1	1.9	21.0	3.3
$9/2_1$	64.1	15.9	1.9	0.4	9.8	3.1
$11/2_2$		27.7	15.3	20.7	21.9	6.4

It is interesting to examine also the structure of the intrinsic state. The wave function of the 7/2 ground state is dominated by the Nilsson orbital [413]7/2, with 92% probability. The dominant value of K is also 7/2, with a probability of 83%. Therefore, the lowest yrast states look very much like strong coupling states. This is probably due to the relatively large deformation.

The particle orbital of the $11/2_2$ is also [413]7/2, but the dominant value of K is 11/2. This difference between K and Ω comes from the core rotation around the quantization axis. The observed anomalous signature splitting in the yrare band is confirmed by the model at a semi-quantitative degree.

V. CONCLUSION

A high-spin level scheme of the very neutron-rich nucleus ^{115}Rh has been built for the first time by analyzing the fission data of ^{252}Cf obtained with Gammasphere. An yrast band with eight new levels and an yrare band with five new level are observed in ^{115}Rh. Based on the fact that the level structure of ^{115}Rh bears a remarkable similarity to those of odd-even $^{107-113}$Rh, the yrast band and yrare bands are proposed to be built on the $7/2^+$ ground state and an $11/2^+$ excitation state, respectively, which is supported by present model calculations.

Systematic studies of neutron-rich even-N Ru, Rh, and Pd isotopes indicate an $N = 68$ effect where the nucleus has the lowest excitation energies. This phenomenon is seen in the yrare bands in odd-even Rh as well. A large signature splitting is observed in the yrast band of ^{115}Rh by plotting the signature splitting function $S(I)$, which follows the systematics that large signature splittings have been found in lighter odd-even Rh isotopes from $A = 107$ to $A = 113$. The previous and present studies in odd-even Rh isotopes with triaxiality show that triaxiality increases from ^{107}Rh to ^{111}Rh and then remains much the same for ^{113,115}Rh. A small but inverted signature splitting in the yrare band is observed.

The experimental excitation energies have been compared to the theoretical results based on the Rigid Triaxial Rotor plus Particle model, with good agreement. This model has successfully described the properties of neutron-rich odd-even Rh, Tc, Nb, and Y isotopes. The deformation parameters fitted to ^{115}Rh are $\epsilon = 0.26$ and $\gamma = 27.5°$. The lowest yrast states are dominated by a $K = 7/2$ component. The intrinsic state is dominated by the particle projection quantum number $\Omega = 7/2$ all along the yrast band, and in the lower half of the yrare sequence. The lower spin states of the yrare band are dominated by $K = 11/2$ components. This high value of K is connected to a shift of the rotational angular momentum towards a principal axis with a lower moment of inertia. Also the strong signature splitting in the yrast band is typical for triaxiality, and this feature is satisfactorily described by the model. The measured gamma branching ratios have been satisfactorily described by the model, which reflect the core structure of the wave functions.

ACKNOWLEDGMENTS

The work at Vanderbilt University, UNIRIB/Oak Ridge Associated Universities, Mississippi State University, and Lawrence Berkeley National Laboratory is supported by the U.S. Department of Energy under Grant and Contract Nos. DE-FG05-88ER40407, DE-AC05-76OR00033, DE-FG02-95ER40939, and DE-AC03-76SF00098. The work at Tsinghua University is supported by the National Natural Science Foundation of China under Grants Nos. 10775078 and 10975082 and by the Major State Basic Research Development Program under Grant No. 2007CB815005. The authors would like to thank Prof. P. von Brentano, Prof. R. V. Jolos, Prof. I. Ragnarsson, Dr. P. Semmes, and Dr. I. Stefanescu for useful discussions and for communicating unpublished computer codes.

[1] J. Skalski, S. Mizutori, and W. Nazarewicz, Nucl. Phys. **A617**, 282 (1997).
[2] J. H. Hamilton *et al.*, Prog. Part. Nucl. Phys. **35**, 635 (1995).
[3] H. Hua, C. Y. Wu, D. Cline, A. B. Hayes, R. Teng, R. M. Clark, P. Fallon, A. Goergen, A. O. Macchiavelli, and K. Vetter, Phys. Rev. C **69**, 014317 (2004).
[4] Y. X. Luo *et al.*, J. Phys. G: Nucl. Part. Phys. **31**, 1303 (2005).
[5] Y. X. Luo et al., Phys. Rev. C **70**, 044310 (2004).
[6] Y. X. Luo *et al.*, Phys. Rev. C **74**, 024308 (2006).
[7] Y. X. Luo *et al.*, Phys. Rev. C **69**, 024315 (2004) and references therein.
[8] Ts. Venkova *et al.*, Eur. Phys. J. A **6**, 405 (1999).
[9] Ts. Venkova *et al.*, Eur. Phys. J. A **15**, 429 (2002).
[10] J. Kurpeta *et al.*, Eur. Phys. J. A **31**, 263 (2007).
[11] J. Äystö *et al.*,Phys. Lett. B **201**, 211 (1988).
[12] D. C. Radford, Nucl. Instrum. Methods Phys. Res. A **361**, 297 (1995).
[13] S. H. Liu *et al.*, (submitted to Phys. Rev. C).
[14] W. B. Walters, E. A. Henry and R. A. Meyer, Phys. Rev. C **29**, 991 (1984).
[15] C. T. Zhang *et al.*, Phys. Rev. Lett. **77**, 3743 (1996).
[16] S. H. Liu, J. H. Hamilton, A. V. Ramayya, J. K. Hwang, A. V. Daniel, G. M. Ter-Akopian, Y. X. Luo, J. O. Rasmussen, S. J. Zhu, and W. C. Ma, Phys. Rev. C **79**, 067303 (2009).
[17] J. K. Hwang *et al.*, Phys. Rev. C **74**, 017303 (2006).
[18] Y. J. Chen *et al.*, Phys. Rev. C **73**, 054316 (2006).
[19] Y. X. Luo *et al.*, Int. J. Mod. Phys. E **18**, 1697 (2009);S. J. Zhu *et al.*, Int. J. Mod. Phys. E **18**, 1717 (2009).
[20] A. Korgul *et al.*, Eur. Phys. J. A **7**, 167 (2000); Y. X. Luo *et al.*, Phys. Rev. C **66**, 014305 (2002); W. Urban, T. Rzaca-Urban, N. Schulz, J. L. Durell, W. R. Phillips, A. G. Smith, B. J. Varley, and I. Ahmad, Eur. Phys. J. A **16**, 303 (2003).
[21] L. Gu *et al.*, Phys. Rev. C **79**, 054317 (2009).
[22] K. Butler-Moore *et al.*, J. Phys. G: Nucl. Part. Phys. **25**, 2253 (1999).
[23] Q. Xu *et al.*, Phys. Rev. C **78**, 064301 (2008).
[24] Y. X. Luo *et al.*, Nucl. Phys. **A838**, 1 (2010).
[25] S. H. Liu, J. H. Hamilton, A. V. Ramayya, Y. X. Luo, J. O. Rasmussen, J. K. Hwang, S. J. Zhu, W. C. Ma, A. V. Daniel, and G. M. Ter-Akopian, Phys. Rev. C **81**, 057304 (2010).
[26] D. Lieberz, A. Gelberg, A. Granderath, P. von Brentano, I. Ragnarsson, and P. B. Semmes, Nucl. Phys. **A529**, 1 (1991).
[27] N. Fotiades *et al.*, Phys. Rev. C **67**, 064304 (2003) and references therein.
[28] N. V. Zamfir and R. F. Casten, Phys. Lett. **B** 260, 265 (1991).
[29] A. Gelberg, D. Lieberz, P. von Brentano, I. Ragnarsson, P.B. Semmes, and I. Wiedenhöver, Nucl. Phys. **A557**, 439c (1993).
[30] J. K. Hwang et al., Phys. Rev. C **65**, 054314 (2002).
[31] R. Bengtsson, H. Frisk, F. R. Mayd and J. A. Pinston, Nucl. Phys. **A415**, 189 (1984).
[32] D. Sohler *et al.*, Phys. Rev. C **71**, 064302 (2005).
[33] I. Deloncle1 *et al.*, Eur. Phys. J. A **8**, 177 (2000).
[34] P. Möller, R. Bengtsson, B. G. Carlsson, P. Olivius, and T. Ichikawa, Phys. Rev. Lett. **97**, 162502 (2006).
[35] J. A. Shannon *et al.*, Phys. Lett. B **336**, 136 (1994).
[36] A. S. Davydov and G. F. Filippov, Nucl. Phys. **2**0, 499 (1960).
[37] S. E. Larsson, G. Leander, and I. Ragnarsson, Nucl. Phys. **A307**, 189 (1978).
[38] I. Ragnarsson and P. Semmes, Hyperf. Int. **43**, 425 (1988).
[39] A. Bohr and B. M. Mottelson, Nuclear Structure, (W. A. Benjamin, Reading, Mass., 1975) vol. II.
[40] T. Yamazaki *et al.*, J. Phys. Soc. Jap., **44**, 1421 (1978).
[41] I. Ragnarsson and P. Semmes, University of Lund, (1991-1999), unpublished.
[42] I. Stefanescu, code ASYRMOIR (private communication, unpublished).